33. AUTHIGENIC BARITE, LEG 41 DEEP SEA DRILLING PROJECT

Walter E. Dean, U.S. Geological Survey, Denver Federal Center, Denver, Colorado
and
B.C. Schreiber, Queens College, City University of New York, Flushing, New York

DESCRIPTION OF BARITE IN DSDP LEG 41 CORES

Rosettes, lenses, and laminae of barite ($BaSO_4$) are common in Lower Cretaceous sediments at Sites 369 and 370 along the continental margin of northwest Africa. Barite at Site 370 occurs as fibrous and feathery crystal aggregates, has a pure composition, and displays no evidence of replacement. However, barite at Site 369 has been replaced by pseudomorphous calcite. Fortunately, there are enough examples in which replacement of barite by calcite has been observed in transition to demonstrate that the calcite was indeed originally barite. The following observations provide insight regarding the origin of barite at these two sites and of deep-sea barite in general.

1) Zones containing barite (or calcite pseudomorphous after barite) commonly occur immediately above thin limestone beds contained within marl-rich sequences. The limestone may be composed of relatively pure, microcrystalline calcite (e.g., Figures 1 and 2), or may simply represent cementation of marl (i.e., an argillaceous limestone or marlstone; Figures 3-6). Both the formation of barite and the cementation of the marl are obviously diagenetic, but it is not always clear which came first. Physical relationships between barite and cement at Site 369 suggest that the two formed more or less simultaneously (e.g., Figures 3-6), although the replacement of barite by calcite may indicate that calcite cementation occurred after formation of barite. At Site 370, barite was occasionally observed to cut across limestone, indicating that barite formed after calcite cement (e.g., Figures 1 and 2). Several excellent examples of partly replaced barite rosettes within limestone at Site 369 indicate that in fact calcite cementation occurred in at least two stages (369-42A-3, 43-46 cm; 369-41A-4, 145-147 cm; Figures 7 and 8). First came the main phase of calcite cementation, then growth of barite rosettes cutting across the limestone, and finally partial or complete replacement of barite by calcite. In all cases in which barite was observed to cut across preexisting rock or sediment, the contacts are sharp physical and chemical boundaries.

2) Barite at both sites occurs in dark-olive, nanno-bearing marl of Aptian to Albian age, containing up to 4% organic carbon. Analyses for organic carbon in samples collected at 10-cm intervals adjacent to several barite zones reveal that barite usually occurs just below an organic-rich zone within the marl (Figures 3 and 5). For example, the average organic carbon concentration in Aptian to Albian marls at Site 369 is about 1.4% ($N=30$, Hole 369A, Cores 39 to 47), but just above a zone containing barite (or calcite pseudomorphous after barite), the organic carbon concentration is usually greater than 3%-4% (Figures 3 and 5).

Barite-bearing organic-rich marls at Sites 369 and 370 are correlative with organic-rich black shales of Aptian to Albian age common at many sites in the Atlantic. The organic-rich Lower Cretaceous sediments may be related to widespread bottom-water stagnation in the juvenile Atlantic Ocean (e.g., Bolli, Ryan, et al., 1975), or may be related to an increased influx of organic debris with resultant fluctuating redox conditions within the sediments (see Dean et al., this volume). The important point here is the association of barite with high organic content of the sediments.

3) Barite at both sites occurs just below a major unconformity. Much of the Cretaceous and lower Tertiary sequence at Site 369 is missing, and sediments that are present apparently accumulated at a slow rate (3.5 to 19 m/m.y.). At least 35 m.y. of the Upper Cretaceous is missing at Site 370, with rapid deposition of turbidites (18 to 35 m/m.y.) above and below the unconformity.

4) Interstitial water salinities increase downward at both sites (Figure 9), probably in response to suspected underlying Jurassic evaporites (see Geochemistry sections in Site 369 and Site 370 Summary Chapters, this volume). Interstitial water salinity at Site 369 increases from 35‰ to 46‰, with most of the increase occurring below the lower Tertiary unconformity (Figure 9). Interstitial water salinity at Site 370 increases from 35‰ to about 60‰. Although the salinity increase at Site 370 is gradual and more or less constant, there is a bulge in both salinity and Ca^{++} curves just below the Cretaceous unconformity and the zone of occurrence of barite (Figure 9).

5) Unreplaced barite is a relatively pure, well-crystallized mineral (Figures 1, 2, 10, and 11; Table 1). The feathery barite crystal aggregates in Core 20, Section 2, Site 370 (Figures 1 and 2) occur within a pure microcrystalline limestone. Figure 2 shows that the barite is slightly higher in Fe, Na, and perhaps Mn, and slightly lower in Mg than adjacent limestone. Church (1970) and Cronan (1974) state that marine barites in general are exceptionally pure. Church (1970) found about one mole percent Sr and less than 0.1 mole percent each of K and Ca in solid solution in barite samples he analyzed. Chesselet et al. (1976) found no Sr in suspended barite crystals in three Atlantic profiles. Microprobe analyses for Sr in barite crystals from Sample 370-20-2, 105-112 cm, range from 0.2 to 1.7

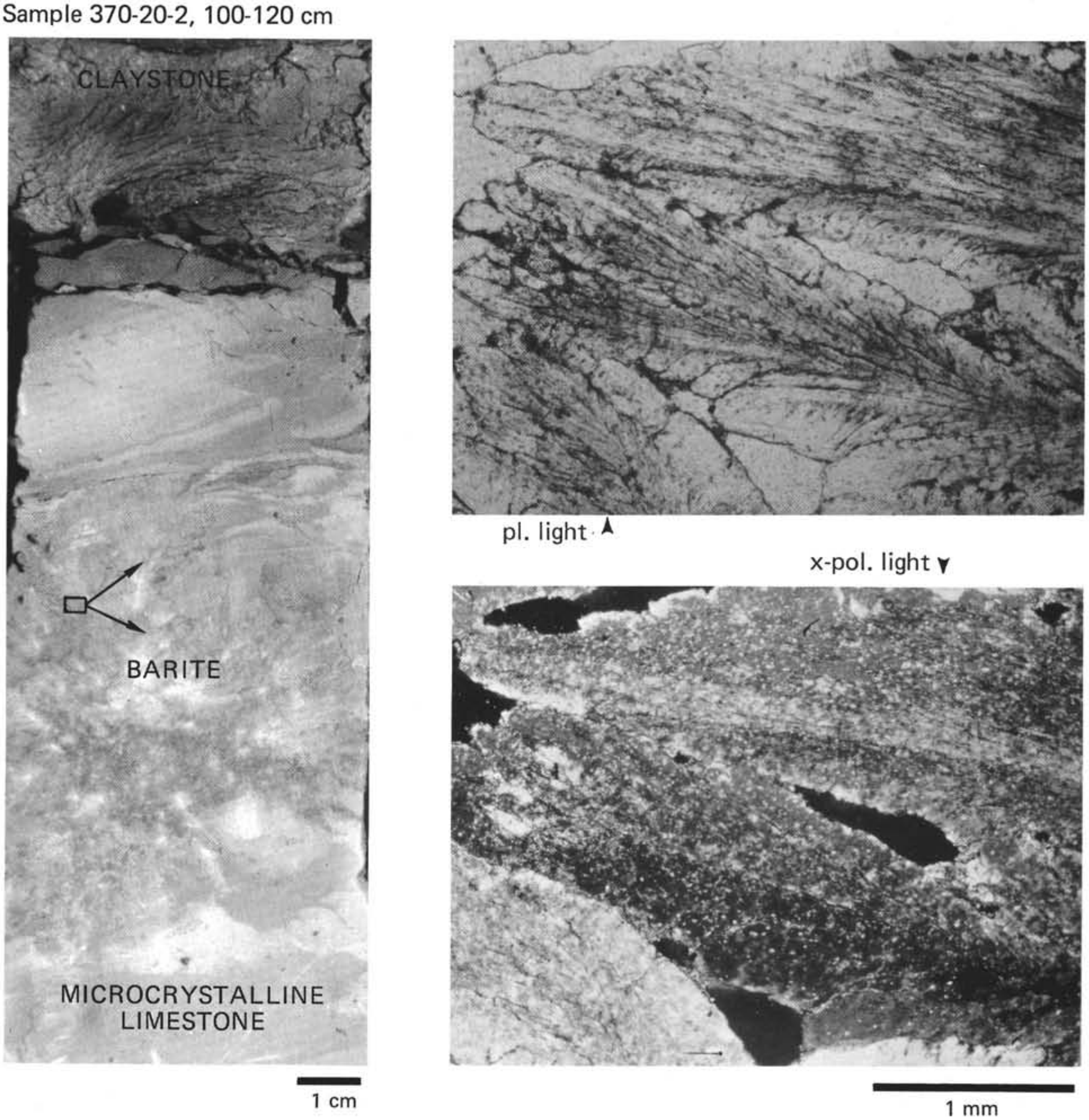

Figure 1. *Core photograph and photomicrographs of barite crystal aggregates in microcrystalline limestone. Sample 370-20-2, 100-120 cm.*

weight percent (N=23). Goldberg et al. (1969) were unable to detect any significant differences in Sr concentrations between marine and continental barites, but did find that continental barites contain considerably less Th and U than deep-sea barites.

OTHER OCCURRENCES OF DEEP-SEA BARITE

Barite is one of the more common authigenic minerals found in deep-sea sediments. It is particularly abundant in sediments from the eastern equatorial and southeastern Pacific, but has been reported in sediments from many other localities. Most deep-sea barite is in the form of small (usually less than 10 μm) euhedral crystals. Nodules of barite as much as 30 cm in diameter are common in sediments from elevated banks in the Sea of Japan, but these apparently formed in isolated seawater "lakes" during Pleistocene glacial intervals and hydrothermal fluids were a source of the Ba (Sakai, 1971). Barite nodules in sediments off the coast of California were described as being of deep-sea hydrothermal origin by Revelle and Emery (1951). However, more recent studies of these nodules by Goldberg et al. (1969) suggest that they originated in either a coastal lagoon or shallower hydrothermal environment and were subsequently transported to their present deep-sea location. Cronan (1974) provides an excellent summary of the literature to about 1972 on the occurrence of deep-sea barite.

In an attempt to expand Cronan's summary of the occurrence of barite in Deep Sea Drilling Project cores, we have compiled X-ray diffraction results for barite as

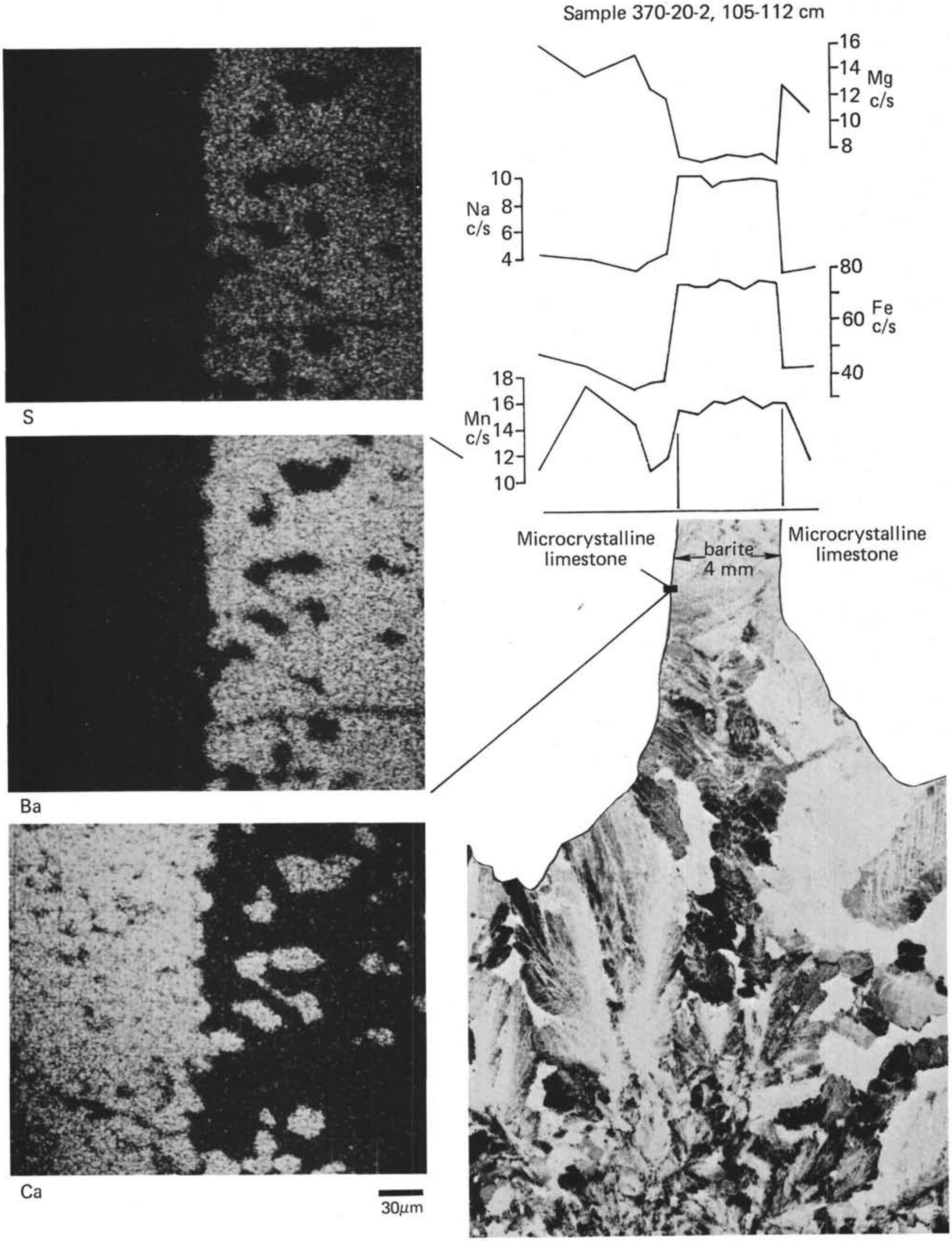

Figure 2. *Electron microprobe X-ray images for S, Ba, and Ca at contact between microcrystalline limestone and barite, Sample 370-20-2, 105-112 cm. Relative concentrations (in counts per second) of Mn, Fe, Na, and Mg are plotted for a single traverse across a "finger" of the barite crystal aggregate in microcrystalline limestone. Photomicrograph made under cross-polarized light.*

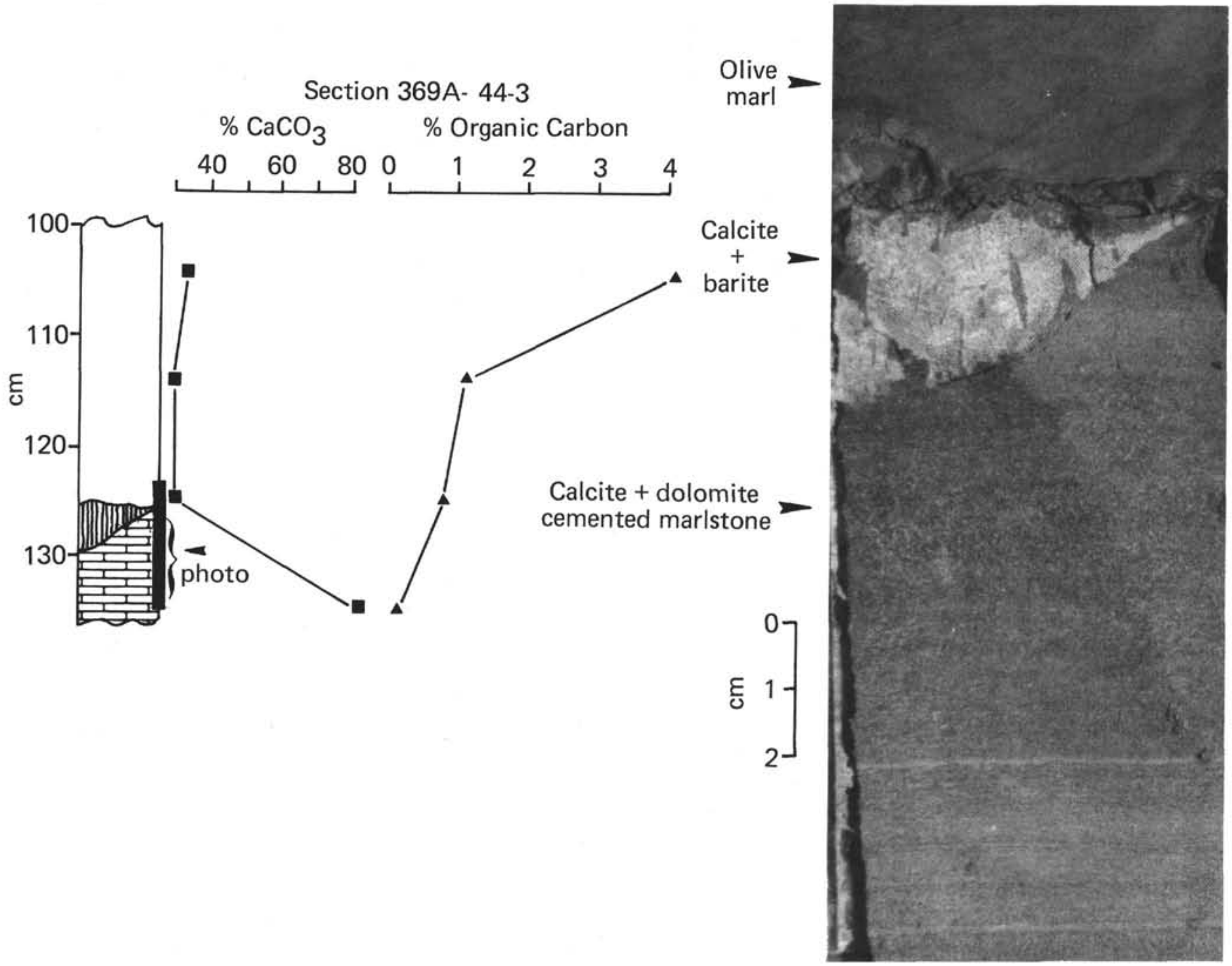

Figure 3. *Core photograph of a lens of calcite pseudomorphous after barite in cemented and uncemented marl. Section 369-44-3. Concentrations of organic carbon and $CaCO_3$ at 10-cm intervals are plotted for the interval 100-130 cm.*

reported in the DSDP Initial Reports volumes through Leg 32, as well as some visual observations from a few more recent legs (Figures 12 and 13; Table 2). Several observations are apparent from this compilation.

1) Barite is far more abundant in cores from the eastern tropical Pacific than from any other area. Undoubtedly, this generalization will change somewhat as additional sites are drilled (e.g., no data yet exists for the southeastern and south-central Pacific), but it does strengthen Cronan's (1974) observation, based on early Deep Sea Drilling Project legs, that the geographic distribution of barite in subsurface sediments is very similar to the reported geographic distribution of barite in surface sediments (e.g., Arrhenius and Bonatti, 1965; Church, 1970).

2) Barite is most abundant in the 2-20 μm size fraction. Crystals larger than this are rare. Church (1970) found that the bulk of barite in surface sediments is microcrystalline, and that rare larger crystals (10-200 μm) were associated with ferromanganese deposits. Chesselet et al. (1976) report that suspended barite in three detailed profiles in the Atlantic shows a log-normal size distribution with a mode of about 0.9 to 1.2 μm.

3) In general, barite is found in older sediments in the Atlantic and Indian oceans than in the Pacific (Figure 13), although this is partly a function of sampling and ages of sediments available to be sampled. Barite is more common in Cretaceous sediments in the Atlantic and Indian Oceans, but in the Pacific barite is more common in Oligocene to Miocene sediments. It is apparent from Figure 13 that there are numerous exceptions to this generality, and perhaps the only permissible conclusion at this time is that barite occurs in sediments of all ages.

4) As another generality with numerous exceptions, barite tends to increase in abundance with depth within a core at a given site. Although this conclusion is not readily apparent from Table 2 and Figure 13, it is apparent from scanning raw data tables in DSDP Initial Reports volumes. This relationship is graphically illustrated in the mineral percentage versus depth histograms that appear in a number of X-ray Mineralogy chapters in DSDP Initial Reports.

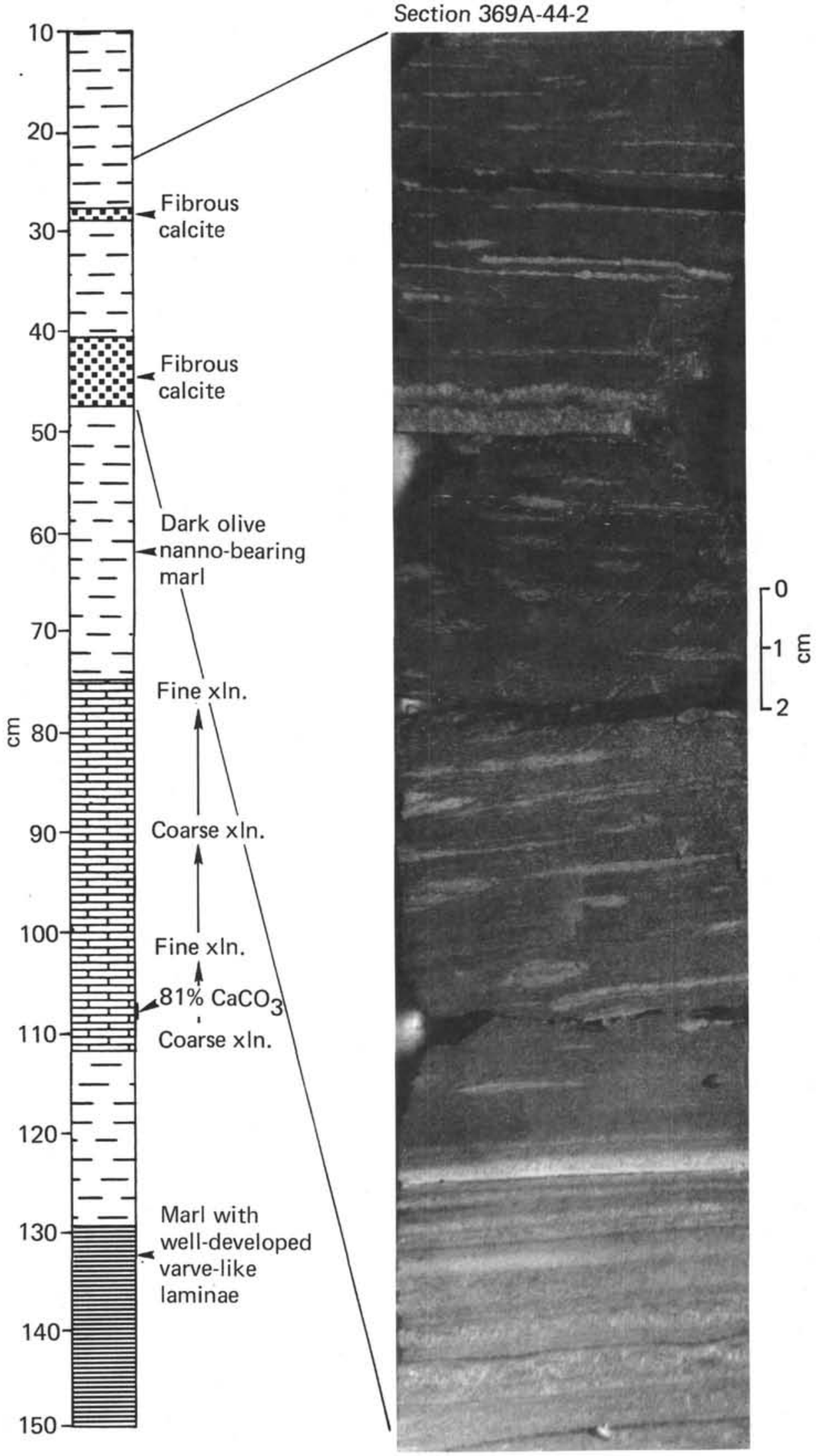

Figure 4. *Core photograph of laminae of fibrous calcite, possibly pseudomorphous after barite, in nanno-bearing marl. Section 369A-44-2.*

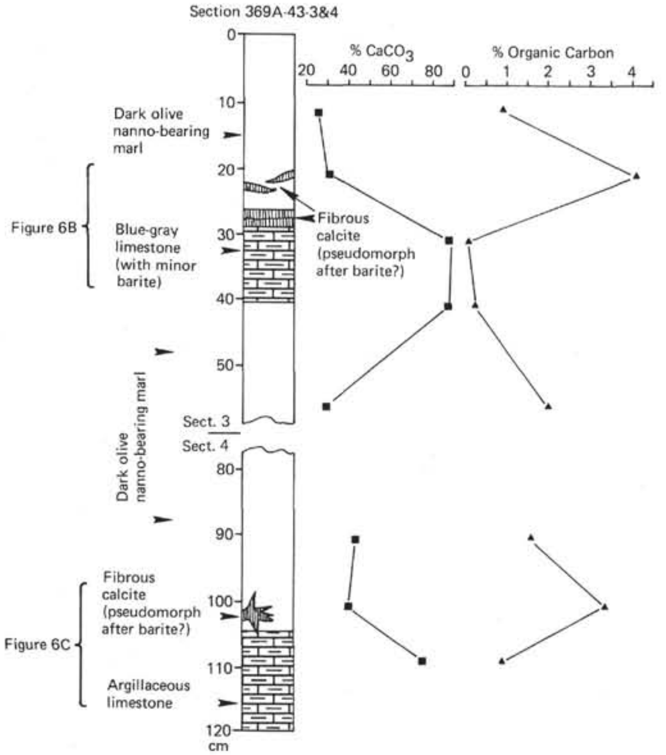

Figure 5. *Plots of concentrations of organic carbon and $CaCO_3$ at 10-cm intervals through nanno-bearing marl and limestone containing calcite possibly pseudomorphous after barite. Sections 369A-43-3 and 4. Photographs of two marl-limestone contacts are shown in Figure 6.*

5) Despite the fact that Church (1970) and Cronan (1974) emphasized the association of barite with calcareous sediments, and that barite in the Pacific is associated with calcareous sediments, there does not appear to be a universal correlation with sediment type. In fact it appears that barite is found in a wide variety of sediment types.

ORIGIN

Most theories regarding the origin of deep-sea barite have invoked volcanic or biogenic processes, or a combination of the two. For example, Arrhenius and Bonatti (1965) concluded that the source of Ba for the formation of barite in the southeastern Pacific is from hydrothermal activity over the East Pacific Rise. Much of the Ba precipitates directly as barite over the rise. As bottom-water masses containing residual dissolved Ba move northward, uptake of Ba by a "curtain of marine organisms" in the equatorial high-productivity zone and subsequent sedimentation as barite produce a concentration of barite in this region. In this way Arrhenius and Bonatti attempted to explain high concentrations of barite in sediments over the East Pacific Rise and in the eastern equatorial Pacific, using the same hydrothermal source of Ba. The barite formed by direct precipitation over the East Pacific Rise is in the form of euhedral crystals, whereas biogenic barite in the equatorial region is in smaller spindle-shaped granules.

Does the majority of deep-sea barite (e.g., the barite in 2-20 μm size fractions of numerous DSDP cores), whether organic or inorganic in origin, form within the water column or within the sediments? Although some barite may be precipitating from seawater, most recent evidence suggests that most deep-sea barite is diagenetic. Chow and Goldberg (1960) and Turekian and Johnson (1965) found that barium concentrations often increase with depth in ocean water. However, more recent investigations by Church and Wolgemuth (1972) show that seawater is apparently undersaturated with respect to barite at all depths, but that pore waters in the east Pacific cores that they analyzed have Ba concentrations at least twice as high as any Pacific bottom water and were at saturation. They concluded that enrichment of Ba in interstitial waters must be diagenetic, probably from oxidation of Ba-rich particulate organic matter.

Evidence for precipitation of barite from seawater is provided by Chesselet et al. (1976), who found fine-grained barite suspended in the upper 3 km of Atlantic, Pacific, and Antarctic waters. Detailed analyses of three Atlantic profiles show that suspended barite is associated either with zones of high surface organic productivity or the Mid-Atlantic Ridge.

The occurrence of barite as large rosettes, laminae, and lenses displacing sediments at DSDP Sites 105, 369, and 370 proves that barite can form diagenetically. In fact, the mounting evidence suggests to us that much, if not most, deep-sea barite is diagenetic. The abundance of barite with depth in DSDP cores, in many cases even increasing with depth, supports a diagenetic origin, or at the very least shows that barite is not diagenetically unstable. Church and Wolgemuth (1972) concluded that because Ba concentrations are greater in sediment pore waters than in overlying seawater, Ba enrichment and barite formation must be diagenetic. Studies of thorium isotopic compositions of marine barites (e.g., Somayajulu and Goldberg, 1966; Goldberg et al., 1969; Church and Bernat, 1972) indicate that barite concentrates Th relative to enclosing sediments, and that the Th concentration in barite tends to decrease with depth in cores. On the basis of this evidence, Church and Bernat (1972) concluded that barite forms diagenetically near the sediment surface. In addition, the unique Th composition of marine barites (high Th concentration, low $^{230}Th/^{232}Th$ ratio) serves to distinguish them from barites that have had a deep-sea hydrothermal origin (lower Th concentration, higher $^{230}Th/^{232}Th$ ratio).

Theories regarding the involvement of organisms in the formation of deep-sea barite range from direct precipitation in protoplasts (e.g., Arrhenius and Bonatti, 1965) to secondary biochemical mechanisms of Ba concentration, transport, and release (e.g., Chow and Goldberg, 1960; Church, 1970; Church and Wolgemuth, 1972). Concentration of Ba by organisms is well known. For example, Bowen (1956) reported Ba concentrations ranging from 450 to 4400 times seawater in a wide variety of marine organisms. Release of this Ba by postmortem decay would provide on the order of 20 to 200 μg Ba per gram dry weight of organic material. Beginning with 1.0 mg of a sediment

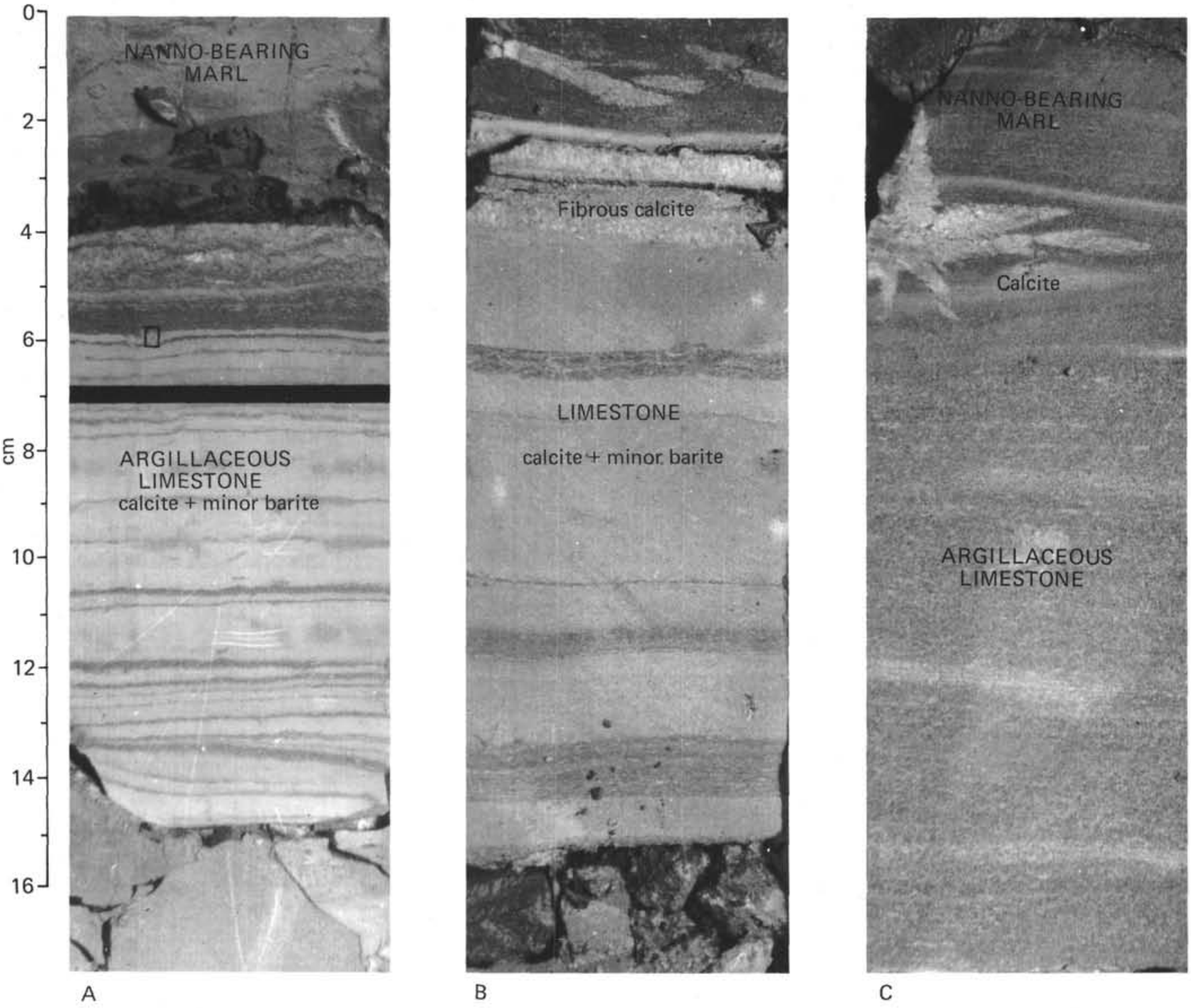

Figure 6. *Core photographs of calcite-cemented zones within nanno-bearing marl. Hole 369A. Calcite possibly pseudomorphous after barite. Photomicrograph of barite rosette partially replaced by calcite (area outlined in core photograph A) is shown in Figure 9. (A) Core 42, Section 3; (B) Core 43, Section 3; (C) Core 43, Section 4.*

containing 1% organic carbon, and assuming that (1) this 1% organic carbon represents 2% dry weight of original organic material, and (2) the original organic material contained 50 μg Ba per gram dry weight (about 10^3 times more Ba than typical equatorial Pacific bottom water), then a barite crystal 7 μm on a side (0.34×10^{-9} cm^3) could be formed from the Ba contained in this 1.0 mg of sediment. In other words, an average deep-sea barite crystal could easily form from as little as 1.0 mg of sediment. On the other hand, it would take all of the Ba in 3×10^3 kg of the same sediment to form a 1.0 cm^3 barite crystal, the same order of magnitude as the barite crystal aggregates found at DSDP Sites 105, 369, and 370. This would be equivalent to a little more than 1.0 m^3 of sediment, but if the sediment contained more than 2% original organic material, or if the organic material contained more than 50 μg Ba per gram organic matter, then the required volume would be proportionally less.

The above mass-balance calculations, plus the frequent association of barite with organic-rich sediments (Church, 1970; this study) and with high productivity zones in the ocean (Arrhenius and Bonatti, 1965; Church, 1970; Chesselet et al., 1976) certainly argue for an organic source for some if not most of the Ba in deep-sea barites. And yet the presence of a sulfate phase in high-organic, pyritic sediments poses a diagenetic redox dilemma if we assume that equilibrium was attained. The presence of pyrite implies that the sediments were reduced (Figure 14), but the presence of barite would imply that the conditions must be sufficiently oxidizing for sulfur to be present as $(SO_4{=})_{aq}$ (Figure 14 and Bjørlykke and Griffin, 1973). The abundance of $(SO_4{=})_{aq}$ relative to $(HS^-)_{aq}$ and/or $(H_2S)_{aq}$ would depend, in part, on the amount of $SO_4{=}$ available and the rate of its reduction by bacteria. What we are seeing is an intermediate product of a dynamic redox system which is certainly not at equilibrium. That

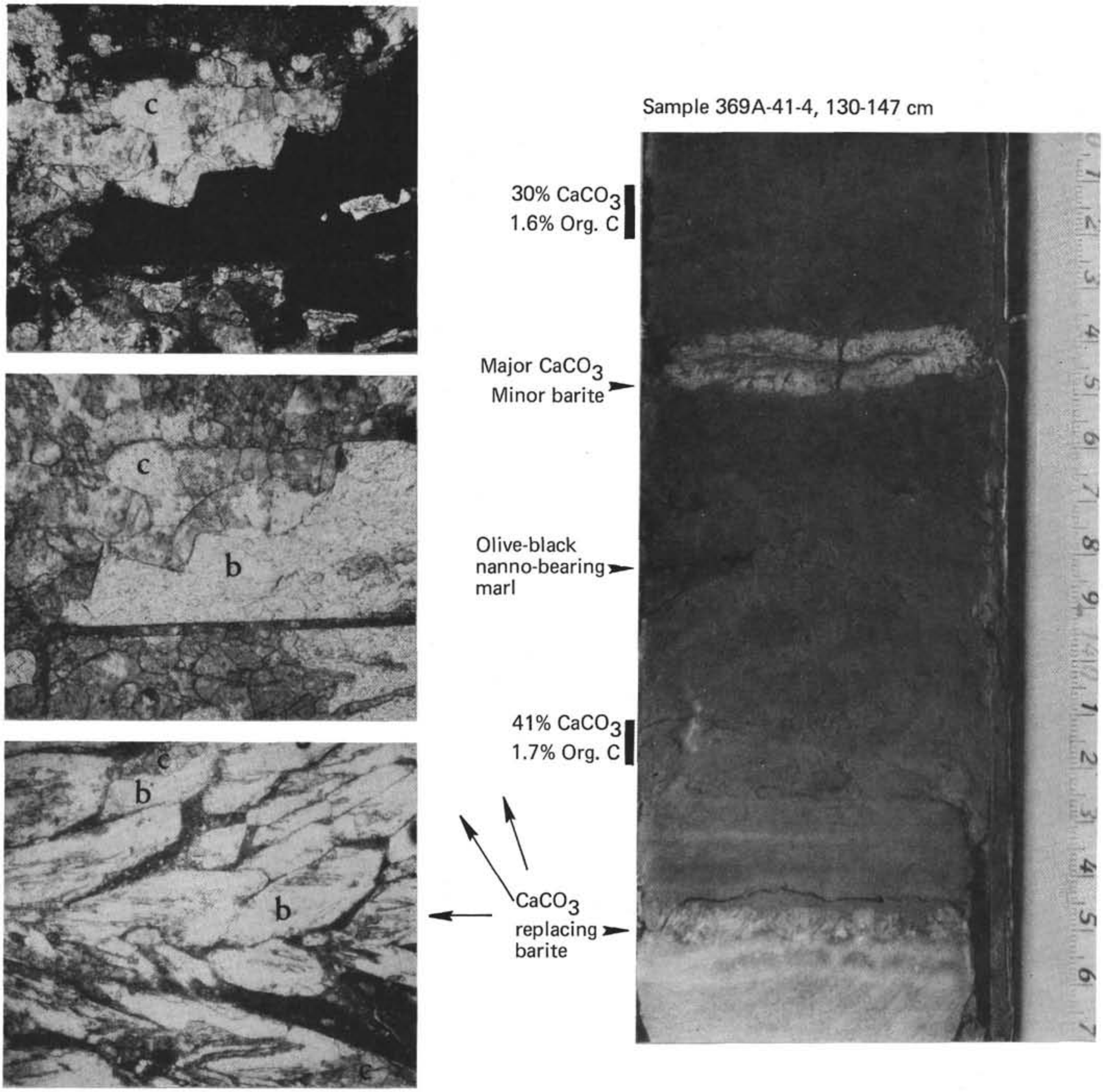

Figure 7. *Core photograph and photomicrographs of barite (b) partially replaced by calcite (c) in nanno-bearing marl. Section 369A-41-4.*

fluctuations in redox conditions probably did occur in the sediments at Sites 369 and 370 is indicated by the proximity of pyrite and barite in the sediments, and the cyclicity in apparent degree of oxidation of the sediments themselves (Dean et al., this volume). An example of probable nonequilibrium diagenetic redox fluctuations is recorded in mineral paragenesis at Sample 367-17-3, 32-34 cm (Figure 15). This part of the section at Site 367 consists of alternating black shale and dark green clay of Late Cretaceous age, interpreted as being the result of cyclic sedimentation of organic material (Dean et al., this volume). Prismatic crystals at a green clay-black shale contact consist of mosaics of calcite containing 5% Mn and 2% Mg, which have been partially replaced by marcasite (Figure 15). The form of the crystal outlines suggests that the original mineral was either gypsum or barite that has been completely replaced by an interlocking mosaic of calcite crystals, which, in turn, has been partially replaced by marcasite. The fluctuating redox story recorded by this paragenetic sequence would be more satisfying if the carbonate phase was siderite rather than calcite (Figure 14). However, electron microprobe analyses show that the calcite is surprisingly low in iron (near

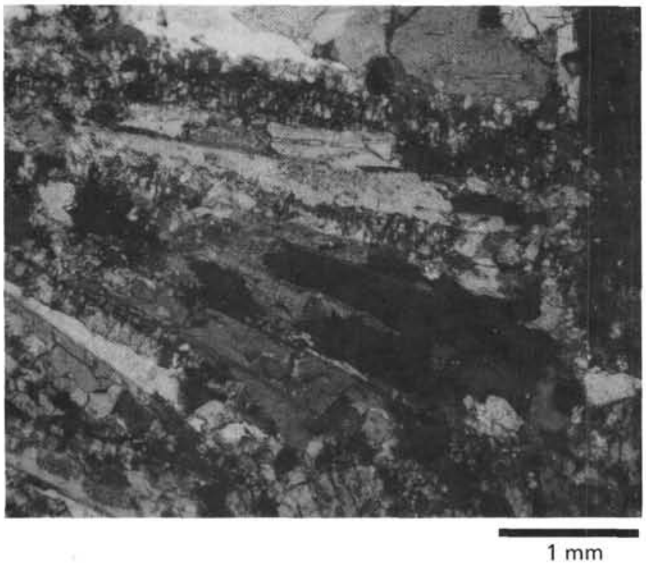

Figure 8. *Photomicrograph (crossed-polarized light) of barite rosette partially replaced by calcite. Sample 369A-42-3, 43-46 cm. (bar = 1mm)*

background), but unusually high in manganese (about 5%). A similar mineral paragenesis, without the intermediate carbonate phase, occurs in Holocene sediments in the Red Sea, where anhydrite crystals have been partially replaced by marcasite (Stephens and Wittkopp, 1969).

The significance of high barite concentrations at Sites 369 and 370, often associated with calcite cementation, may be related to supply of calcium and sulfate from underlying evaporites, as suggested by increasing interstitial-water salinity at Site 369 and increasing interstitial-water salinity and Ca^{++} concentration at Site 370. Church (1970) has suggested that one function of the common association of deep-sea barite with calcium carbonate is pH buffering, maintaining a high pH, so that $(SO_4{=})_{aq}$ would be stable even under slightly reducing conditions (Figure 14).

A more ancient analog of the deep-sea barite and organic association has been described by Bjørlykke and Griffin (1973) in Ordovician graptolitic shales from Norway. In these shales, original barite has been replaced by quartz, calcite, pyrite, and Ba-rich feldspar. According to the Bjørlykke and Griffin model for this occurrence, barite formed by oxidation of preexisting pyrite under oxidizing conditions during temporary pauses in sedimentation. With subsequent diagenesis under reducing conditions in high-organic sediments, barite was dissolved and replaced by quartz, calcite, pyrite, and feldspar. They also point out the importance of carbonate in maintaining a high pH, thereby permitting greater stability of barite under slightly reducing conditions. Applying this model to the

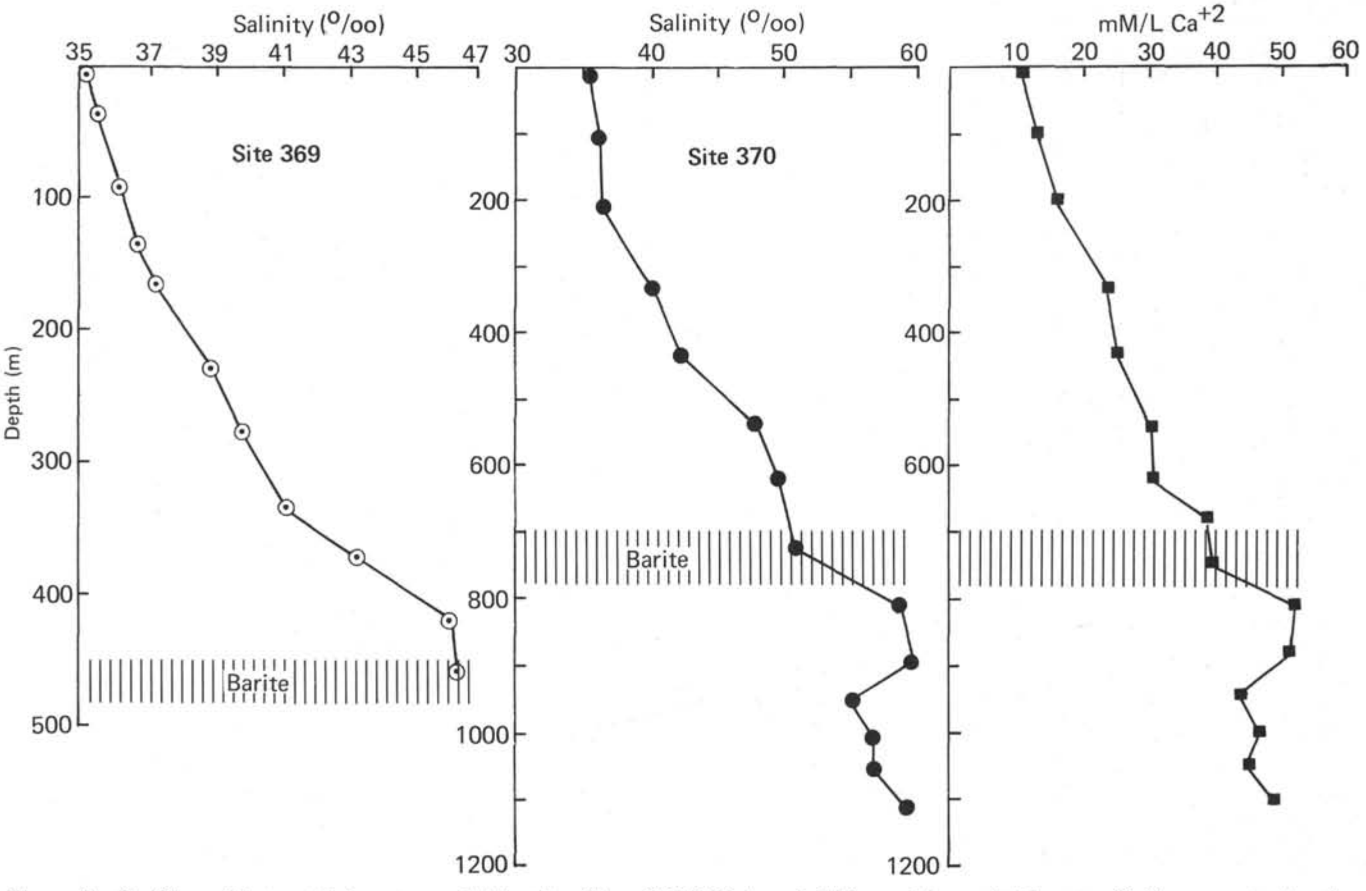

Figure 9. *Profiles of interstitial water salinities for Sites 369/369A and 370, and interstitial water Ca^{++} concentration for Site 370.*

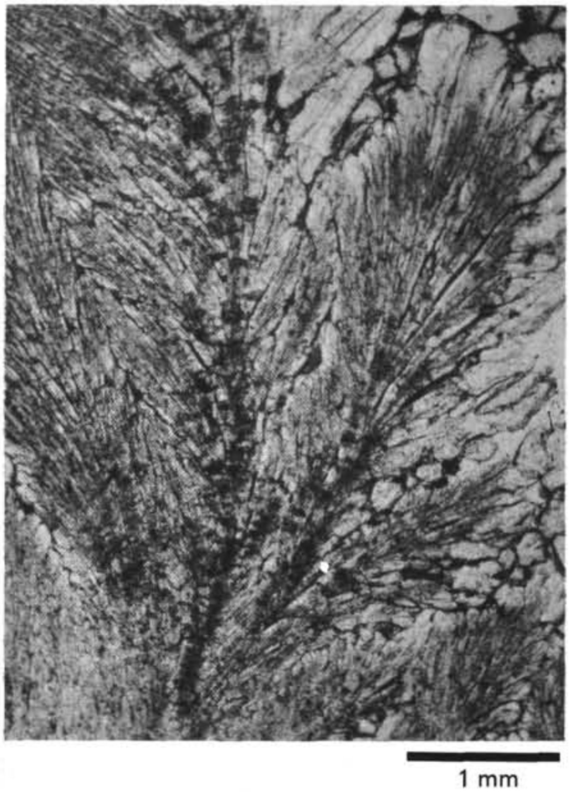

Figure 10. *Photomicrograph (plane light) of feathery barite crystal aggregate in nanno-bearing shale. Section 370-22-3.*

occurrence of barite in Leg 41 sediments, oxidizing conditions during pauses in sedimentation would explain the association of barite with major unconformities and would suggest that the hiatuses are not necessarily due to erosion. If the main source of sulfate for barite formation at Sites 369 and 370 was from underlying evaporites, oxidation of pyrite would not be necessary as an additional sulfate source as in the Bjørlykke and Griffin model, but it would certainly help.

CONCLUSIONS

Barite, or calcite pseudomorphous after barite, observed at Sites 369 and 370, occurs in high-organic, Lower Cretaceous sediments immediately below a major unconformity and is associated with marked increases in interstitial water salinities. We conclude that the barite formed diagenetically under oxidizing or slightly reducing conditions in sediments exposed at the sediment-water interface for long periods of time during pauses in sedimentation. The main source of Ba was from oxidation of organic matter. Because of long exposure of the sediments at the sediment-water interface, because the sediments contain pyrite, and because of the association with increasing interstitial water salinity gradients, three sources of sulfate are suggested: (1) diffusion of overlying seawater sulfate into the sediments to replace sulfate consumed by barite formation and/or sulfate reduction, (2) oxidation of preexisting pyrite, and (3) upward diffusion of sulfate from solution of evaporites at depth.

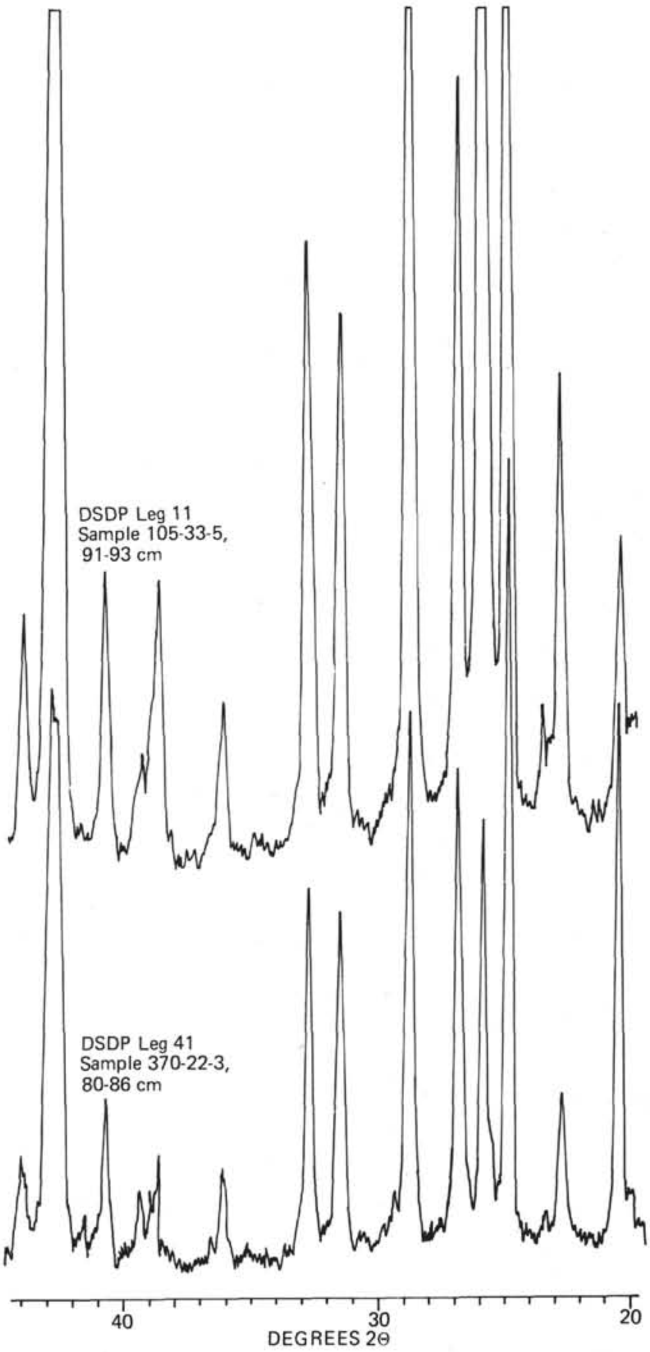

Figure 11. *X-ray diffraction patterns of barite crystals from Sites 105 (Leg 11) and 370 (Leg 41).*

Reports of deep-sea barite in surface sediments and in Deep Sea Drilling Project cores show that fine-grained barite is common in organic-rich sediments of just about every type and age.

ACKNOWLEDGMENTS

We thank Willard S. Moore, Department of Geology, University of South Carolina; Martin Goldhaber, U.S. Geological Survey, Denver; and James Gardner, U.S. Geological Survey, Menlo Park, for reviewing this paper.

TABLE 1
X-Ray Diffraction *d*-Spacings for Barite Crystals, Sample 370-22-3, 80-86 cm Compared With *d*-Spacings From Barite in ASTM Standard X-Ray Powder Diffraction File No. 5-0448

ASTM Barite[a]			DSDP 41-370-22-3, 80-86 cm
d (Å)	°2θ	I/I$_1$	Degrees 2θ
4.44	20.00	17	20.1
4.34	20.46	36	20.5
3.90	22.78	57	22.9
3.77	23.60	12	
3.576	24.90	31	24.9
3.442	25.88	100	25.9
3.317	26.85	67	26.9
3.101	28.79	97	28.7
			28.8
2.834	31.54	53	31.6
2.734	32.75	16	32.8
2.726	32.82	47	32.9
2.481	36.20	14	36.2
2.444	36.84	2	
2.322	28.78	15	28.8
2.303	39.11	6	39.2
2.281	39.50	7	39.5
2.209	40.81	27	40.6
			40.8
2.120	42.61	80	42.7
2.104	42.95	76	43.0
2.056	44.0	23	44.0
			44.15
1.947	46.6	1	
1.930	47.0	7	
1.857	49.0	16	

[a] Powder diffraction file no. 5-0448; sample from Mallinckrodt Chemical Works.

REFERENCES

Arrhenius, G. and Bonatti, E., 1965. Neptunism and volcanism in the ocean. *In* Sears, M. (Ed.), Progress in oceanography, v. 3: London (Pergamon Press), p. 7-22.

Bjørlykke, K.O. and Griffin, W.L., 1973. Barium feldspars in Ordovician sediments, Oslo Region, Norway: J. Sediment. Petrol., v. 43, p. 461-465.

Bolli, H.M., Ryan, W.B.F., et al., 1975. Basins and margins of the eastern South Atlantic: Geotimes, June, p. 22-24.

Bowen, H.J.M., 1956. Strontium and barium in seawater and marine organisms: J. Marine Bio. Assoc. U.K., v. 35, p. 451-460.

Chesselet, R., Jedwab, J., Darcourt, C., and Dehairs, F., 1976. Barite as discrete suspended particles in the Atlantic Ocean (abs.): Trans. Am. Geophys. Union, v. 57, p. 255.

Chow, T.J. and Goldberg, E.D., 1960. On the marine geochemistry of barium: Geochim. Cosmochim. Acta, v. 20, p. 192-198.

Church, T.M., 1970. Marine barite: Unpublished Ph.D. Dissertation, Univ. California, San Diego, 133 p.

Church, T.M. and Bernat, M., 1972. Thorium and uranium in marine barite: Earth Planet. Sci. Lett., v. 14, p. 139-144.

Church, T.M. and Wolgemuth, K., 1972. Marine barite saturation: Earth Planet. Sci. Lett., v. 15, p. 35-44.

Cronan, D.S., 1974. Authigenic minerals in deep-sea sediments. *In* Goldberg, E.D. (Ed.), The sea, v. 5: New York (Wiley-Interscience), p. 491-525.

Garrels, R.M. and Christ, C.L., 1965. Solutions, minerals, and equilibria: New York (Harper and Row), 450 p.

Goldberg, E.D., Somayajulu, B.L.K., and Galloway, J., 1969. Differences between barites of marine and continental origins: Geochim. Cosmochim. Acta, v. 33, p. 287-289.

Revelle, R. and Emery, K.O., 1951. Barite concretions from the ocean floor: Geol. Soc. Am. Bull., v. 62, p. 707-724.

Sakai, H., 1971. Sulfur and oxygen isotopic study of barite concretions from banks in the Japan Sea off the Northeast Honshu, Japan: Geochim. J., v. 5, p. 79-93.

Somayajulu, B.L.J. and Goldberg, E.D., 1966. Thorium and uranium isotopes in seawater and sediments: Earth Planet. Sci. Lett., v. 1, p. 102-106.

Stephens, J.D. and Wittkopp, R.W., 1969. Microscopic and electron beam microprobe study of sulfide minerals in Red Sea mud samples. *In* Degens, E.T. and Ross, D.A. (Eds.), Hot brines and Recent heavy metal deposits in the Red Sea: New York (Springer-Verlag), p. 441-447.

Turekian, K.K. and Johnson, D.G., 1966. The barium distribution in sea water: Geochim. Cosmochim. Acta, v. 30, p. 1153-1174.

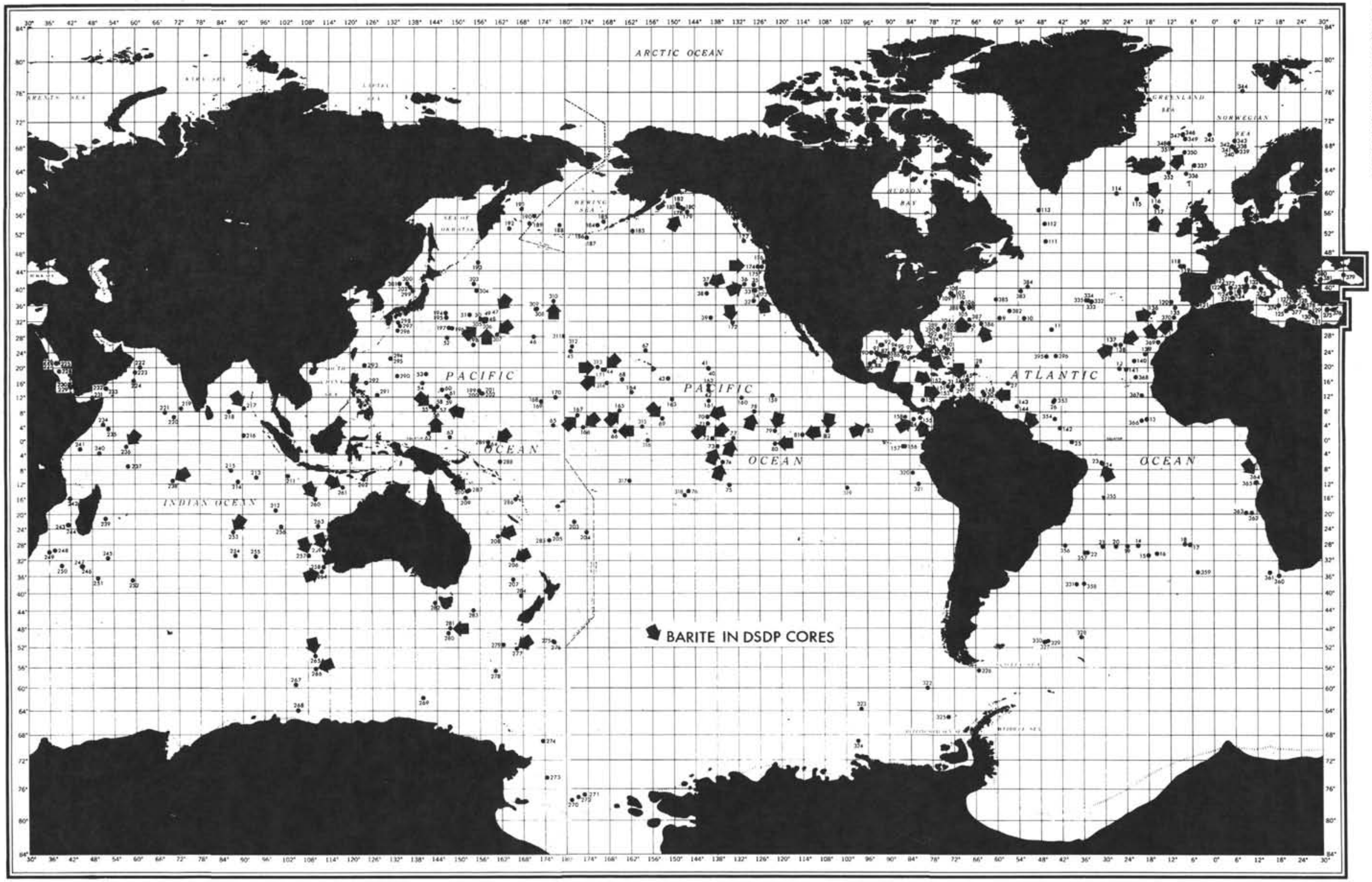

Figure 12. *Map of DSDP Sites showing those for which barite has been reported either from X-ray diffraction results of visual descriptions.*

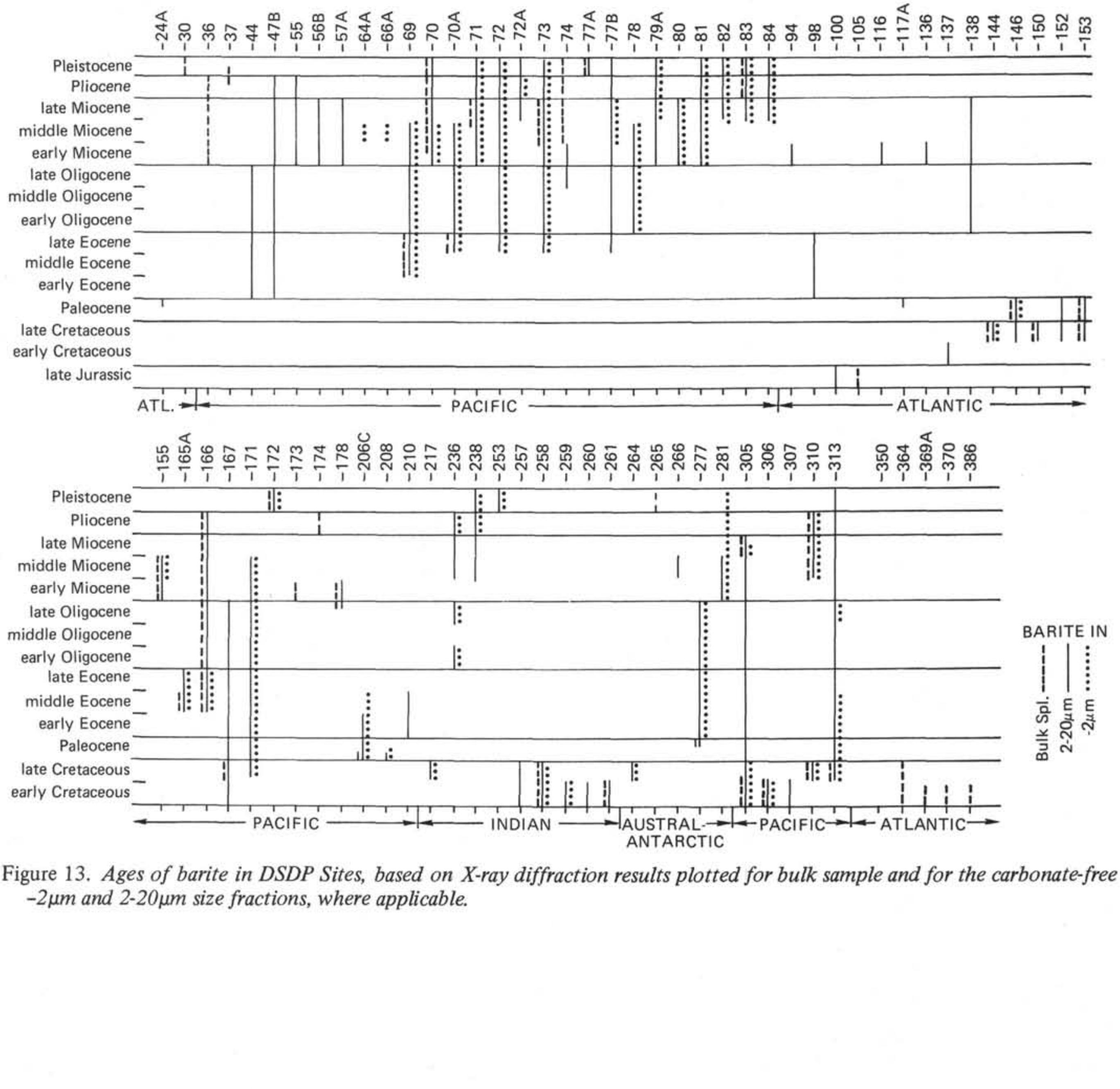

Figure 13. *Ages of barite in DSDP Sites, based on X-ray diffraction results plotted for bulk sample and for the carbonate-free -2μm and 2-20μm size fractions, where applicable.*

TABLE 2
Barite in X-Ray Diffraction Results of Deep Sea Drilling Project Samples

Leg	Site	Depth (m)	Core	Age	Size Fraction	Barite (%)
4	24A	5148	4	Late Paleocene	2-20 μm	4%
	30	1218	1	Pleistocene	Bulk	4%
	30	1218	2	Pleistocene	Bulk	7%
5	36	3273	9-13	Miocene and Pliocene	Bulk	5-12% in most samples
	37	4682	1-2	Pliocene and Pleistocene	Bulk	11-25% in all samples
6	44	1478		Eocene and Oligocene	2-20 μm	4-30% in all samples
	47B	2689	3-7	Eocene to Pliocene	2-20 μm	1-3% in most samples
	55	2850	3-4	Miocene and Pliocene	2-20 μm	7-10% in most samples
	55	2850	6; 8		2-20 μm	11%
	56B	2508	2-5	Miocene	2-20 μm	3-38% in most samples
	57A	3300	1	Miocene	2-20 μm	6%
7	64	2060	4	Middle Miocene	<2 μm	4%
	64A	2060	4	Middle Miocene	<2 μm	13%
	66A	5310	8	Miccle Miocene	<2 μm	10%
8	69	4978	6	Miccle Eocene	Bulk	100%
	69	4978	2-6	Middle Eocene to middle Miocene	2-20 μm	The major xln. phase in all samples
	69	4978	3-5	Early Oligocene to middle Miocene	<2 μm	5-16% in most samples
	69A	4978	9-12	Middle and late Eocene	Bulk	27-61% in most samples
	69A	4978	1-11	Late Eocene to early Miocene	2-20 μm	The major xln. phase in all samples
	69A	4978	1-10	Late Eocene to early Miocene	<2 μm	1-18% in most samples
	70	5059	1-5	Middle Miocene to Quaternary	Bulk	2-17% in most samples
	70	5059	1-12	Early Miocene to Quaternary	2-20 μm	Present to dominant in most samples
	70	5059	3-12	Early and middle Miocene	<2 μm	5-57% in most samples
	70A	5059	28-30	Late Eocene	Bulk	3-37% in most samples
	70A	5059	1-30	Late Eocene to early Miocene	2-20 μm	The major xln. phase in all samples
	70A	5059	1-30	Late Eocene to early Miocene	<2 μm	2-67% in all samples (most > 10%)
	71	4419	3	Late Miocene	Bulk	3%
	71	4419	1-48	Late Oligocene to Pleistocene	2-20 μm	The major xln. phase in all samples
	71	4419	1-48	Late Oligocene to Pleistocene	<2 μm	3-67% in all samples (most > 10%)
	72	4326	2-11	Late Eocene to Quaternary	2-20 μm	The major xln. phase in all samples
	72	4326	1-5; 7 9-11	Late Eocene to Quaternary	<2 μm	10-74% in most samples
	72A	4326	1-6	Late Miocene to Quaternary	2-20 μm	The major xln. phase in all samples
	72A	4326	2-4	Pliocene	<2 μm	6-20% in most samples
	73	4387	8-9	Middle and late Miocene	Bulk	2-14% in most samples
	73	4387	1-20	Late Eocene to Pleistocene	2-20 μm	The major xln. phase in all samples
	73	4387	2-20	Late Eocene to Pleistocene	<2 μm	3-40% in most samples
	74	4431	1-4	Middle Miocene to Pleistocene	Bulk	4-8% in most samples
	74	4431	4; 9	Late Oligocene; early Miocene	2-20 μm	Present to dominant in most samples
9	77A	4291	1	Pleistocene	Bulk	Major
	77A	4291	1	Pleistocene	2-20 μm	The major xln. phase in all samples
	77A	4291	1	Pleistocene	<2 μm	18%
	77B	4291	52	Late Eocene	Bulk	15%
	77B	4291	1-52	Late Eocene to Pleistocene	2-20 μm	The major xln. phase in most samples
	77B	4291	17; 19; 21	Middle and late Miocene	<2 μm	100%
			others		<2 μm	Up to % in most samples (most > 10%)
	79	4574	1-16	Early Miocene to Pleistocene	2-20 μm	The major xln. phase in all samples
	79	4574	1; 5-14	Pleistocene; early and middle Miocene	<2 μm	Up to 17% in most samples (most > 10%)
	79A	4574	1-4	Early Miocene to Pleistocene	2-20 μm	The major xln. phase in all samples
	79A	4574	1-3	Late Miocene to Pleistocene	<2 μm	Up to 7% in all samples
	80	4411	1-5	Miocene	2-20 μm	The major xln. phase in all samples
	80	4411	2-4	Miocene	<2 μm	2-11% in most samples
	80A	4411	2-5	Early Miocene to early Pliocene	2-20 μm	The major xln. phase in all samples
	80A	4411	4-5	Early Miocene	<2 μm	Ca. 3%
	81	3865	1-6	Early Miocene to Pleistocene	2-20 μm	The major xln. phase in all samples
	81	3865	1-6	Early Miocene to Pleistocene	<2 μm	62% in Core 1; < 10% in all other spls.
	82	3707	1-6	Late Miocene to Pleistocene	2-20 μm	Present to dominant in all samples
	82	3707	1-5	Late Miocene to Pleistocene	<2 μm	6-25% in most samples
	82A	3707	1-3	Early Pliocene to Pleistocene	2-20 μm	The major xln. phase in all samples
	82A	3707	1-3	Early Pliocene to Pleistocene	<2 μm	1-5% in all samples
	83	3646	2-4	Early Pliocene to Pleistocene	Bulk	3-5% in most samples
	83	3646	1-7	Late Miocene to Pleistocene	2-20 μm	The major xln. phase in all samples
	83	3646	1; 3; 5-7	Late Miocene to Pleistocene	<2 μm	2-10% in most samples

TABLE 2 – *Continued*

Leg	Site	Depth (m)	Core	Age	Size Fraction	Barite (%)
9	83A	3646	1-12	Late Miocene to Pleistocene	Bulk	Up to 5% in most samples
	83A	3646	1-15	Late Miocene to Pleistocene	2-20 μm	Present to dominant in all samples
	83A	3646	5-12	Late Miocene to late Pliocene	<2 μm	2-24% in most samples
	84	3096	10-28	Late Miocene to late Pliocene	2-20 μm	Present in most samples
	84	3096	8; 24; 27	Late Miocene to Pleistocene	<2 μm	2-4% in 3 samples
	78	4378	1-35	Early Oligocene to middle Miocene	2-20 μm	The major xln. phase in all samples
	78	4378	1-32	Early Oligocene to middle Miocene	<2 μm	Up to 13% in most samples
10	94	1793	9	Early Miocene	2-20 μm	2-8% in most samples
	94	1793	10	Early Miocene	2-20 μm	8-25% in most samples
11	98	2769	7; 9	Eocene	2-20 μm	Present (2-8%)
	100	5325	7	Late Jurassic	2-20 μm	Abundant (8-25%)
	105	5251	33	Late Jurassic	Bulk	Barite lens (Section 5, 91-93 cm)
12	116	1151	12	Early Miocene	2-20 μm	5%
	116	1151	20	Early Miocene	2-20 μm	2%
	117A	1038	6	Late Paleocene	Bulk	14%
14	144	2957	3	Late Cretaceous	Bulk	2%
	144	2957	3	Late Cretaceous	2-20 μm	16%
	144	2957	3	Late Createceous	<2 μm	2%
	136	4169	4	Early Miocene	2-20 μm	2%
	137	5361	14	Early Cretaceous	2-20 μm	1%
	137	5361	16	Early Cretaceous	2-20 μm	4%
	138	5288	2	Oligocene and Miocene (?)	2-20 μm	5%
15	146	3949	8-13	Plaoecene	Bulk	1-5% in all samples
	146	3949	8-39	Late Cretaceous and Paleocene	2-20 μm	1-13% in most samples (most < 5%)
	146	3949	8-13	Paleocene	<2 μm	1-3% in most samples
	150	4545	10	Late Cretaceous	Bulk	3%
	150	4545	10	Late Createous	2-20 μm	13%
	152	3899	3-22	Late Cretaceous and Paleocene	2-20 μm	2-15% in most samples
	153	3932	10-12 15	Late Createous and Paleocene	Bulk	2-4% in most samples
	153	3932	9-17	Late Createous and Paleocene	2-20 μm	6-41% in most samples (most < 10%)
16	155	2752	3-5	Early and middle Miocene	Bulk	2-5% in most samples
	155	2752	3-9	Early and miccle Miocene	2-20 μm	2-22% in most samples
	155	2752	6-9	Middle Miocene	<2 μm	2-4% in most samples
	157	2591	9-10	Pliocene and Pleistocene	Bulk	2-3% in all samples
	157	2591	18	Pliocene	Bulk	1%
	157	2591	1-39	Late Miocene to Holocene	2-20 μm	6-46% in most samples (most < 10%)
	157	2591	1-16	Late Pliocene to Holocene	<2 μm	3-100% in most samples (100% in Core 16, 144-153 meters sub-bottom)
	158	1953	24-25	Middle and late Miocene	Bulk	1-3% in all samples
	158	1953	1-33	Middle Miocene to Holocene	2-20 μm	3-69% in most samples (most < 20%)
	158	1953	5-32	Middle Miocene to Pleistocene	<2 μm	3-19% in most samples
	159	4484	1-10	Early Miocene to Holocene	Bulk	1-5% in most samples
	158	4484	1-10	Early Miocene to Holocene	2-20 μm	1-13% in most samples
	158	4484	3-10	Early Miocene to Holocene	<2 μm	4-6% in most samples
	160	4940	1-5	Early Miocene to Pleistocene	Bulk	1-10% in most samples
	160	4940	1-12	Oligocene to Pleistocene	2-20 μm	3-23% in most samples (most < 10%)
	160	4940	3-12	Oligocene to Pleistocene	<2 μm	2-10% in most samples
	161	4939	1-2	Early Miocene	Bulk	1-20% in most samples
	161	4939	10-12	Late Eocene	Bulk	1-20% in most samples
	161	4939	1-14	Middle Eocene to early Miocene	2-20 μm	5-33% in all samples (most 15%)
	161	4939	1-14	Middle Eocene to early Miocene	<2 μm	2-10% in most samples
	162	4854	3-5	Late Eocene	2-20 μm	3-5% in most samples
	163	5320	3; 7; 10; 1A	Middle Miocene to late Oligocene	Bulk	4-81% in most samples (most < 10%)
17	164	5485	25	Early Cretaceous	Bulk	52%
	164	5485	25	Early Createous	2-20 μm	16%
	165	5040	1-2	Late Oligocene to early Miocene	Bulk	3-4% in 3 of 5 samples
	165A	5040	9; 12-13	Middle Eocene	Bulk	4-50% in most samples
	165A	5040	2	Late Eocene	2-20 μm	8%
	165A	5040	6-13	Middle and late Eocene	2-20 μm	4-83% in all samples (most < 20%)
	165A	5040	6-13	Middle and late Eocene	<2 μm	2-57% in most samples
	166	4950	2-16	Middle Eocene to Pliocene	Bulk	4-35% in most samples
	166	4950	2-16	Middle Eocene to Pliocene	2-20 μm	2-38% in most samples
	166	4950	12-16	Middle and late Eocene	<2 μm	2-8% in most samples

TABLE 2 – *Continued*

Leg	Site	Depth (m)	Core	Age	Size Fraction	Barite (%)
17	167	3166	66	Late Creatceous	Bulk	3%
	167	3166	11-93	Late Jurassic to Oligocene	2-20 μm	2-38% in 6 of 8 samples
	171	2283	2-19	Late Cretaceous to middle Miocene	2-20 μm	1-21% in all samples
	171	2283	25	Late Cretaceous	2-20 μm	3%
	171	2283	2-19	Late Creatceous to middle Miocene	<2 μm	1-12% in 8 of 9 samples
18	172	4768	1	Quaternary	Bulk	3%
	172	4768	1	Quaternary	2-20 μm	2%
	172	4768	1	Quaternary	<2 μm	3%
	173	2927	30	Early Miocene	Bulk	7%
	174	2815	37	Pliocene	Bulk	2%
	178	4218	54; 57	Early Miocene	Bulk	2-22% in all samples
	178	4218	54; 57	Early Miocene	2-20 μm	4-14% in all samples
21	206C	3196	21	Early and middle Paleocene	Bulk	1%
	206C	3196	15-21	Early Paleocene to early Eocene	2-20 μm	3-50% in most samples (most < 10%)
	206C	3196	17-21	Early Paleocene to middle Eocene	<2 μm	1-5% in most samples
	208	1545	30-34	Early Paleocene	2-20 μm	2-34% in 3 samples
	208	1545	30-34	Early Paleocene	<2 μm	2-15% in 3 samples
	210	4643	44-49	Early and middle Eocene	2-20 μm	Ca. 2% in most samples
22	217	3030	34	Late Cretaceous	2-20 μm	5%
	217	3030	37	Late Cretaceous	2-20 μm	21%
	217	3030	34	Late Cretaceous	<2 μm	2%
	217	3030	37	Late Cretaceous	<2 μm	3%
24	236	4487	3	Pliocene	2-20 μm	5%
	236	4487	6	Late Miocene	2-20 μm	2%
	236	4487	15	Middle Miocene	2-20 μm	2%
	236	4487	22	Late Oligocene	2-20 μm	35%
	236	4487	25	Early Oligocene	2-20 μm	49%
	236	4487	3	Pliocene	<2 μm	3%
	236	4487	22	Late Oligocene	<2 μm	2%
	236	4487	25	Early Oligocene	<2 μm	3%
	238	2832	1-38	Quaternary to middle Miocene	2-20 μm	4-45% in all samples (9)
	238	2832	1-14	Quaternary to early Pliocene	<2 μm	7-13% in all samples (7)
26	253	1962	1	Quaternary	2-20 μm	7%
	253	1962	1	Quaternary	<2 μm	9%
	257	5278	9	Cretaceous(?)	2-20 μm	1%
	258	2793	10-15	Cretaceous	Bulk	1-4% in all samples
	258	2793	6-21	Cretaceous	2-20 μm	2-15% in all samples
	258	2793	6-18	Cretaceous	<2 μm	2-37% in all samples
27	259	4712	27	Early Cretaceous	2-20 μm	1%
	259	4712	30-31	Early Cretaceous	2-20 μm	2-3%
	259	4712	30	Early Cretaceous	<2 μm	1%
	260	5709	15	Early Cretaceous	2-20 μm	2%
	261	5687	23-31	Early Cretaceous	Bulk	1-9% in most samples
	261	5687	23-31	Early Cretaceous	2-20 μm	1-9% in most samples
28	264	2873	11	Late Cretaceous	Bulk	1-2%
	264	2873	11	Late Cretaceous	2-20 μm	5-13%
	265	3582	2	Pleistocene	Bulk	1%
	266	4173	15-17	Middle Miocene	2-20 μm	2-4%
29	277	1214	44	Late Paleocene	Bulk	1%
	277	1214	3-5	Middle and late Oligocene	2-20 μm	3-6% in 3 samples
	277	1214	19-46	Middle Paleocene and early Oligocene	2-20 μm	2-23% in most samples (most < 10%)
	277	1213	3-5	Middle and late Oligocene	<2 μm	2-5% in 3 samples
	277	1214	19-46	Middle Paleocene and early Oligocene	<2 μm	1-11% in most samples
	281	1591	6-11	Early and middle Miocene	2-20 μm	9-50% in 3 samples
	281	1591	2	Pliocene and Pleistocene	<2 μm	3%
	281	1591	6-12	Miocene	<2 μm	5-15% in all samples
	281A	1591	3	Late Miocene to early Pliocene	<2 μm	5%
32	305	2903	5-6	Late Miocene	Bulk	1-2% in 4 samples
	305	2903	65-66	Early Cretaceous	Bulk	1-2%
	305	2903	5-59	Early Cretaceous to late Miocene	2-20 μm	1-19% in most samples
	305	2903	66	Early Cretaceous	2-20 μm	3%
	305	2903	5-6	Late Miocene	<2 μm	1-2% in 3 samples
	305	2903	16	Late Cretaceous	<2 μm	2%

TABLE 2 – *Continued*

Leg	Site	Depth (m)	Core	Age	Size Fraction	Barite (%)
32	305	2903	23	Late Cretaceous	<2 μm	1%
	305	2903	59	Early Cretaceous	<2 μm	1%
	305	2903	66	Early Cretaceous	<2 μm	2%
	306	3399	21	Early Cretaceous	Bulk	1%
	306	3399	36	Early Cretaceous	Bulk	2%
	306	3399	40	Early Cretaceous	Bulk	3%
	306	3399	21-40	Early Cretaceous	2-20 μm	3-34% in all samples
	306	3399	29-40	Early Cretaceous	<2 μm	1-3% in all samples
	307	5696	11	Early Cretaceous	2-20 μm	7%
	310	3516	5-9	Middle Miocene to Pliocene	Bulk	1-4% in most samples
	310	3516	17	Early Cretaceous	Bulk	29%
	310	3516	5-9	Middle Miocene to Pliocene	2-20 μm	1-6% in most samples
	310	3516	17	Early Cretaceous	2-20 μm	28%
	310	3516	5-9	Middle Miocene to Pliocene	<2 μm	1-2% in most samples
	310	3516	17	Early Cretaceous	<2 μm	7%
	311	5775	1	Oligocene or younger	<2 μm	2%
	313	3484	15	Late Cretaceous	Bulk	2%
	313	3484	1-42	Late Cretaceous to Quaternary	2-20 μm	2-36% in most samples (most < 10%)
	313	3484	3	Late Oligocene	<2 μm	3%
	313	3484	7-42	Late Cretaceous to middle Eocene	<2 μ m	1-10% in most samples
38	350	3484	14		Bulk	Visual – 1-2% in smear slide 14-2, 30 cm
40	364	2448	21-23	Cretaceous	Bulk	Visual –
	364	2448	38-41	Early Cretaceous	Bulk	Visual
41	369A	1760	43-46	Early Cretaceous	Bulk	Visual + X-ray; rosettes and layers
	370	4216	20-27	Early Cretaceous	Bulk	Visual + X-ray; rosettes and layers
43	386	4782	64	Early Cretaceous	Bulk	Visual – 1-15% in smear slides

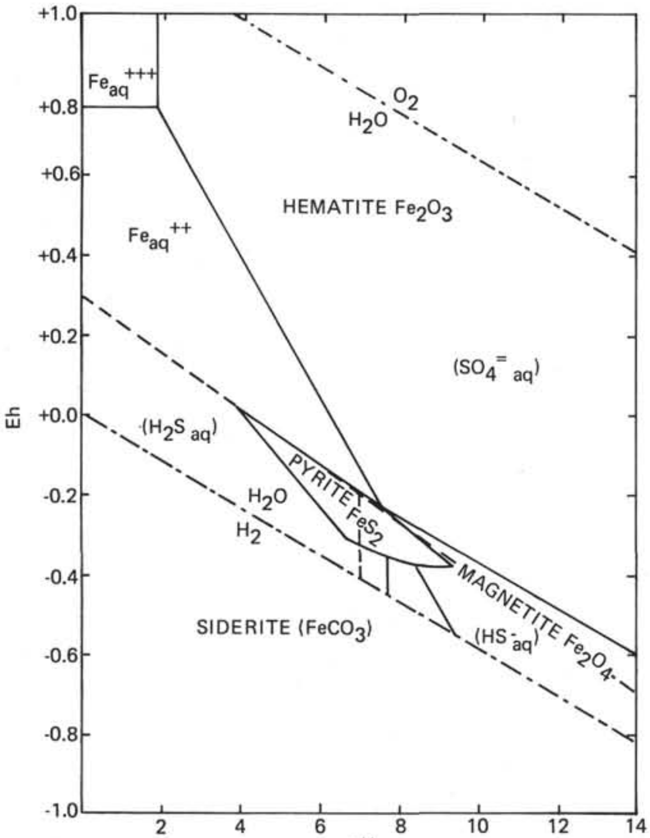

Figure 14. *Stability relations of iron oxides, sulfides, and carbonate in water at 25°C and 1 atm. total pressure. Total dissolved S = 10^{-6}; total dissolved carbonate = 10^{-2}. Stablility fields for dissolved sulfer species are superimposed in dashed lines (modified from Garrels and Christ, 1965).*

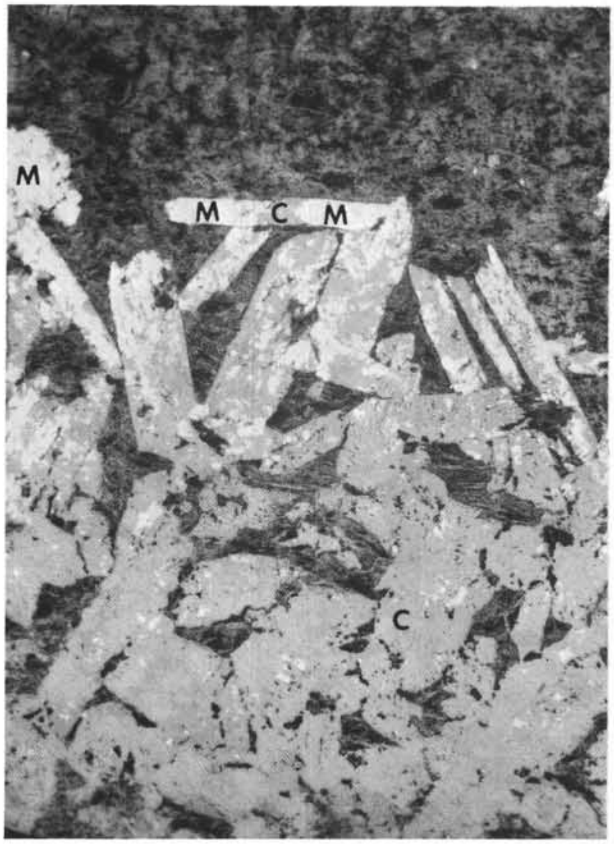

Figure 15. *Core photograph and reflected-light photomicrograph of calcite (C) pseudomorphous after gypsum or barite(?), partially replaced by marcasite (M) at contact between black and green organic-rich shales. Section 367-17-3.*